Peer review status:

This is a non-peer-reviewed preprint submitted to EarthArXiv.

The Condensation Radiation of Water Vapor Drives Diurnal Temperature Range Patterns

Prof. Zhou Shaoxiang

School of Energy Power and Mechanical Engineering of North China

Electric Power University

Beinonglu 2, Zhuxinzhuang, Changping, Beijing (102206), China

Email: zsx@mcepu.edu.cn

2026.06.14

The Condensation Radiation of Water Vapor Drives Diurnal Temperature Range

Zhou Shaoxiang

School of Energy Power and Mechanical Engineering

of North China Electric Power University

Beinonglu 2, Zhuxinzhuang, Changping, Beijing (102206), China.

Email: zsx@mcepu.edu.cn

Abstract: The global distribution and variation of the Diurnal Temperature Range (DTR) remain "an essential knowledge gap" in our understanding of climate dynamics in IPCC assessment reports. This study introduces the radiative mechanism of water vapor condensation as a novel physical driver of DTR dynamics. Contrary to classical heat conduction theory, which assumes latent heat transfers via temperature gradients, we demonstrate that condensation in near-thermal-equilibrium moist air cannot release heat conductively without violating the Second Law of Thermodynamics. Instead, latent heat is released directly via characteristic infrared radiation (Condensation Radiation). This radiative energy propagates over long distances and acts as a primary driver of the nighttime greenhouse effect. Quantitatively, the latent heat associated with global precipitation (~78 W/m²) exceeds anthropogenic heat emissions by three orders of magnitude. Using global publicly available data and case studies (e.g., precipitation events in Beijing), we show that higher condensation intensity - driven by evaporation, humidity, and geography - reduces DTR. This explains the observed spatial and temporal patterns: smaller DTR in coastal regions than inland, at low latitudes than high latitudes, and in summer than winter. Ultimately, the proposed mechanism offers a robust

framework for reconciling long-standing inconsistencies in DTR trends under global warming.

Key Words: Diurnal temperature range; Phase transition radiation; Chemical potential; Phase equilibrium; Greenhouse effect.

1 Introduction

The Diurnal Temperature Range (DTR), defined as the difference between daily maximum (T_{max}) and minimum (T_{min}) temperatures, serves as a critical fingerprint of climate system dynamics. Unlike mean temperature, DTR variations are highly sensitive to cloud cover, humidity, and atmosphere processes. Therefore, it has received widespread attention (Karl et al., 1993; Sun et al., 2019; Xu et al., 2025). However, since research on DTR has not obtained satisfactory answers, the Intergovernmental Panel on Climate Change (IPCC) series of assessment reports has been unable to provide appropriate explanations. The Technical Summary of the Fourth Assessment Report (AR4) identified changes in DTR as a key uncertainty (Solomon et al., 2007; Thorne et al., 2016a). The Fifth Assessment Report (AR5) concluded that understanding of DTR changes is only of "medium confidence" (Hartmann et al., 2013; Thorne et al., 2016a). The Sixth Assessment Report (AR6) explicitly identifies DTR trends as an 'essential knowledge gap' (Gulev et al., 2021; Xu et al., 2025). Since the IPCC assessment reports summarize publicly available academic research results, it can be said that research on the global distribution and variation of DTR has been stagnant. This study presents a paradigm shift by introducing new phenomena and physical mechanisms.

2 The Physical Mechanism about Condensation Radiation

Potter and Hoffman (1968) reported on the experiments conducted in 1965 that the integrated intensity was four times higher than Plank's radiation in the range of 1 - 4 μm wavelength, with the peak radiation intensity exceeding blackbody radiation by over 100 times near 1.54 μm

(Tatartchenko, 2010); therefore, they concluded that "the latent heat of vaporization was radiated directly by the steam condensing into the liquid state." Nichols and Lamar (1968), through comparative analysis, confirmed the discovery of strong infrared radiation sources in the 8 - 14 μm wavelength range at the bottom sides of forming cumulus clouds, but the actual origin of the radiation is still uncertain. Mestvirishvili et al. (1977) detected strong infrared radiation at wavelengths of 4 - 8 μm and 28 - 40 μm, respectively, during the condensation of water vapor (presumably under room temperature conditions) and water chilling crystallization (at 0℃ and below), and proposed that such effects exist in all first-order phase transitions. Carlon (1970, 1979) also discovered extremely strong 8 - 14 μm infrared absorption and emission in cooling fine water aerosols, fogs and clouds. Sall and Smirnov (2000) found that "the intensity of the above-thermal radiation depends on melt cooling conditions," indicating a highly positive correlation between phase transition radiation intensity and condensation intensity. Perel'man and Tatartchenko (2008) conducted a theoretical analysis of the physical mechanism and concluded that "characteristic radiation corresponding to the first order phase transitions in more ordered states exists and can remove out the latent energy of transition; this phenomenon, for the first time, ascertains the internal conformity between the thermodynamic and spectroscopic magnitudes." Tatartchenko (2008) described their experiments concerning recording of the characteristic spectra during sapphire (A_2O_3) crystallization from the melt. Sapphire is transparent over a wide range of the spectrum from infrared to ultraviolet, due to the extremely high temperature (2050℃). Wang et al. (2010) proposed a two-level transition model to explain the radiative transfer mechanism of water vapor condensation radiation and theoretically studied the spectral distribution of the water vapor condensation radiation source function. Tatartchenko (2010, 2012) analyzed and summarized a series of previously published articles, and pointed out that these anomalous infrared characteristic radiations (IRCRs) should originate from latent heat of phase transitions. He also reported that many recorded atmospheric infrared radiation sources appeared to be the result of water crystallization, condensation, and sublimation during fog and

cloud formation processes. Klimenko and Mareev (2018) detected abnormally high-intensity ultra-high frequency (UHF) radio noise as a front passed the observation site, and confirmed that there were no powerful radio emission sources within the antenna's field of view. In fact, accompanying the movement of the front (the precipitation process), low-temperature cloud droplets from upper altitudes descend, causing water vapor in the lower layer moist air to condense onto these cloud droplets; the radiative release of latent heat should be the source of the anomalous radiation from the front.

Furthermore, based on thermodynamic theoretical analysis, it is also demonstrated that the condensation of water vapor into clouds can only release latent heat through radiation (Zhou, 2008). The reasoning is as follows:

(1) Water vapor evaporates from the Earth's surface, mixes into the air and diffuses to high altitudes, forming almost homogeneous local moist air. The components of the moist air tend to be in thermal equilibrium with each other.

(2) The condition for water vapor to condense at high altitudes is for the relative humidity of the moist air to reach 100%. If the concentration of aerosol particles acting as condensation nuclei is insufficient, condensation can typically only proceed when the water vapor is in a supercooled state at its saturation pressure.

(3) In studies concerning the release of latent heat from water vapor condensation in the atmosphere, moist air containing liquid droplets that is approximately in thermodynamic equilibrium is a crucial subject of investigation (Mason, 1975; Wang, 2013); under such a condition, the chemical potential of the water vapor is approximately equal to that of the cloud (liquid) droplets (Zhou, 2008), which aligns with Gibbs phase rule.

(4) According to the principles of heat transfer, a temperature difference is required as the driving force for any engineering heat transfer process. A typical example is the condensation of water vapor and the removal of latent heat, which usually take place on a cold wall. A cooler fluid flowing on the opposite side of the wall carries away the latent heat and maintain the continuity

of condensation (Janna, 2009). However, regarding the release of latent heat during the process of water vapor condensing into clouds, we face an irreconcilable contradiction: for water vapor to condense onto the surface of cloud droplets, the droplet temperature must be lower than that of the water vapor to satisfy requirement of the Second Law of Thermodynamics. However, cloud droplets themselves cannot absorb all latent heat. If it is required to transfer latent heat to the surrounding atmosphere through thermal conduction, the surface temperature of the cloud droplet must be higher than that of the surrounding atmosphere. This is equivalent to requiring low-temperature water vapor to condense on the surface of high-temperature cloud droplets, which conflicts with the second law of thermodynamics.

(5) Since the phase transition of water vapor condensation is an isothermal and isobaric process, it implies that the condensation of water vapor on the cloud droplet surface cannot cause its temperature to rise above that of the surrounding atmosphere (which includes the water vapor). In other words, the necessary driving force for heat conduction (heat transfer temperature difference) cannot be formed between cloud droplets and the surrounding moist air.

(6) The condensation of water vapor into clouds at high altitudes is a natural phenomenon, during which latent heat is definitely released. Therefore, our view is that since latent heat cannot be released through temperature difference-driven heat conduction, it can only be released through radiation (Zhou, 2008).

(7) The consequence of latent heat being released through radiation is that it can propagate over much longer distances. The sources of infrared characteristic radiation in the atmosphere detected by Nichols and Lamar (1968), Tatartchenko et al. (2012), and others, as well as the anomalous UHF signals from moving fronts described by Klimenko and Mareev (2018), align perfectly with this physical mechanism and can be regarded as evidence supporting this view.

Given that water vapor primarily condenses during the night, the radiative release of latent heat is to be considered as the nighttime atmospheric greenhouse effect. In classical theory, however, the heat conduction equation for latent heat release, $[L(dm/dt) = 4\pi r k_{\mathrm{a}}(T_r - T_\infty)]$

(Mason, 1975; Andrews, 2010), is essentially identical to Newton's Law of Cooling used in engineering heat transfer, $[dQ/dt = kA(T - T_\infty)]$ (Janna, 2009). But the problem is that the latter is grounded in the context of fossil fuel combustion, where the temperature difference of heat transfer between the hot object and the atmosphere genuinely exists. In contrast, the temperature difference $(T_r - T_\infty)$ between the cloud droplet surface and the surrounding atmosphere in the former is purely imaginary. Not only that, both approaches treat the atmosphere as a heat reservoir, which is essentially equivalent to assuming that the atmospheric temperature remains constant even when heat is absorbed (T_∞ =constant). However, the latent heat released by water vapor condensation in the atmosphere exceeds the heat generated by fossil fuel combustion by more than three orders of magnitude, and its potential impact on atmospheric temperature is incomparable to that of anthropogenic fossil fuel use. In other words, this default assumption is fundamentally untenable, i.e., this heat conduction equation used to calculate the latent heat release is invalid.

The problem is that, according to the classical theory of heat conduction equations, the condensation of water vapor into clouds occurs at specific altitudes, and its impact is limited to local areas without affecting surface air temperatures. This understanding is, of course, incorrect (Zhou, 2008) and is the fundamental reason why the diurnal temperature range (DTR) has become an essential knowledge gap. In the following text, we will apply the radiative characteristics of water vapor condensation to explain the global distribution and variation of DTR.

It should be noted that the condensation radiation of water vapor in the atmosphere is the first step in the nighttime release of solar energy stored during the day, playing a decisive role on the DTR both quantitatively and chronologically. The supercooling of water vapor and cloud droplets reduces the latent heat released by condensation and freezing respectively, but it does not alter the radiative mode of phase change. The processes such as turbulence within clouds, molecular collisions, and atmospheric convection are all accompanied by the energy transfer of long-wave radiation, which even includes some condensation of water vapor and evaporation. Yet, despite

the added complexity, none of these processes can assume a dominant role.

3 The Intensity Characteristics of Water Vapor Condensation Radiation in the Atmosphere

The physical mechanism that the latent heat of water vapor condensation is released via radiation may not be easily understood, yet it is readily experienced in daily life. In fact, whenever precipitation is approaching, the air temperature typically rises noticeably. In the case of an impending summer storm, the weather often signals its arrival with an unusually muggy and sultry sensation. This occurs because the precipitation process involves the descent of high-altitude cold cloud systems. As raindrops fall through the lower layer of moist air, they cause water vapor to condense on them, and latent heat is released in the way of radiation. These signals arrive before the actual precipitation, allowing people to sense it in advance. It is precisely this mechanism that drives the anomalous UHF signals associated with moving fronts (Klimenko and Mareev, 2018). Meanwhile, just before a rainstorm, the relative humidity of the local surface air usually increases significantly, which enhances the heating effect of water vapor condensation radiation and intensifies the sensation of mugginess.

The IPCC Third Assessment Report (TAR) reports that "the long-term global mean precipitation of 984 mm/yr implies a vertically integrated mean heating rate of 78 $\mathrm{W/m^2}$", (Stocker et al., 2001; Kiehl and Trenberth, 1997), a value averaged over 24 hours a day throughout the year. Numerically, the latent heat from this precipitation amounts to 1.254×10^6 EJ, which is 2,445.4 times the 512.8 EJ of global fossil fuel consumption in 2024 (*Statistical Review of World Energy 2025* by Energy Institute (EI)). The release of both these heat quantities spans the cyclical changes of the seasons. The former could raise the overall atmospheric temperature by 237℃, while the latte's effect would be only 0.097℃. In the context of engineering heat transfer involving fossil fuel utilization, treating the atmosphere as a heat reservoir presents no substantial issues, i.e., Newton's Law of Cooling holds true. However, for the condensation of water vapor

into clouds, such a significant temperature rise clearly indicates that treating the atmosphere as a heat reservoir for latent heat release is incorrect. That is to say, the heat conduction equation for latent heat release in classical theory does not hold.

Given that the radiative release of latent heat from condensation of water vapor into clouds is an atmospheric greenhouse effect primarily occurring at night, it influences surface air temperatures on the night side of the Earth, thereby becoming the decisive factor in the global distribution and variation of the diurnal temperature range (DTR). In fact, the latent heat from global mean precipitation could theoretically warm the entire night-side atmosphere by 948°C. Considering that only about 50% of the latent heat released by condensation may radiate toward the surface, this implies that the global DTR could decrease by approximately 1.3°C as a result. Due to significant geographical and seasonal variations in the evaporation and condensation of water, its actual impact varies greatly across the globe.

Since condensation of water vapor into clouds does not immediately result in precipitation, the formation of precipitation usually requires accumulation over multiple days. During this period, there must be a process where clouds partially evaporate or even completely dissipate during the day (as shown in Figure 1) and regenerate at night due to recondensation. Therefore, the actual radiant energy emitted by the condensation of water vapor in the atmosphere should far exceed the calculated 78 W/m² based on global mean precipitation, and its impact should be even greater.

Fig.1 Evaporation and Dissipation of Clouds (Beijing, October 13, 2007, 16:13-16:15 PM)

The diurnal variations of incoming solar radiation drive the alternating cycle of evaporation and condensation within the Earth's atmosphere system, while its seasonal variations cause this process to exhibit cyclical quantitative changes across different regions. Consequently, the intensity of water vapor condensation in the atmosphere should be higher at night than during the day, higher in summer than in winter, higher over oceans than over land, and higher at low latitudes than at high latitudes. This provides a scientific basis for our analysis of the global distribution and variability of DTR.

4 The Radiative Characteristics of Water Vapor Condensation and the Global Distribution of DTR

Based on the intensity characteristics of water vapor condensation radiation in the atmosphere, we can draw the following inferences regarding the global distribution and variations of DTR: it is smaller in coastal regions than in inland areas, smaller at low latitudes than at high latitudes, and smaller in summer than in winter (see the analysis in section 5.2). This is because these regions and seasons experience greater surface water evaporation, leading to a larger amount of water vapor condensation and, consequently, a greater radiative release of latent heat. However, it is important to note that the diurnal variation in solar radiation at the Earth's poles is minimal, especially during the polar night in winter and the polar day in summer. The conventional concept of DTR is no longer suitable for describing climate changes there, even though actual temperature differences between day and night may still exist.

Fig.2 (Sun X et al., 2021) and Fig.3 (Vinnarasi, 2017) illustrate the annual mean DTR distributions in East Asia and India, respectively, which generally align with the inferences mentioned above. Additionally, according to Barkan et al. (2020), the DTR on the Mediterranean coast of Israel is significantly smaller than that in the inland areas. As noted by Makowski et al.

(2008), Iceland, located in the central North Atlantic, has the lowest DTR in Europe, and the United Kingdom also exhibits a relatively low DTR. Katavoutas et al. (2023) reported that coastal cities such as Stockholm, Nice, and Barcelona have lower DTRs, whereas cities located farther from the coast tend to have larger DTRs. The North Atlantic Drift and the Westerlies exert a significant influence on the European climate. Furthermore, according to Sun D et al. (2006), the western and central regions of the United States are relatively dry, while the eastern and northwestern coastal regions are more humid; consequently, the DTR along the eastern and northwestern coasts is significantly lower than that of the inland areas, with the highest DTRs found in the western deserts and grasslands.

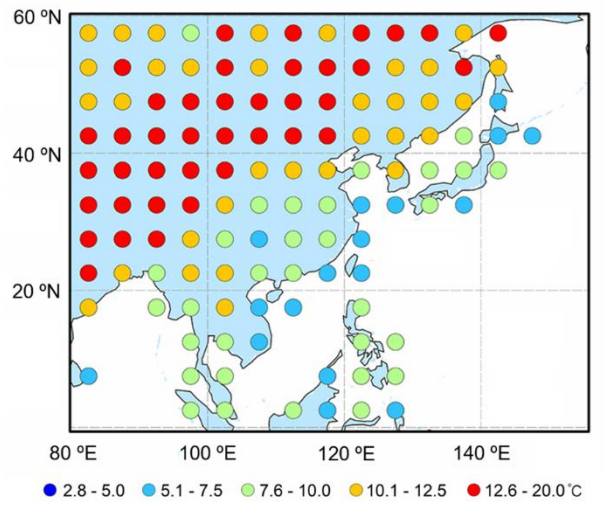

Fig.2 Distribution of Annual Mean DTR in East Asia

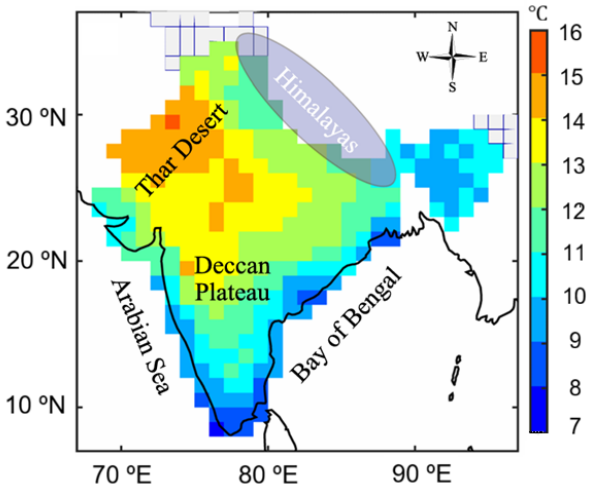

Fig.3 Distribution of Annual Mean DTR in India

Conventional wisdom holds that the maintenance of surface temperature depends on the balance of radiative energy (Manabe and Wetherald, 1967), following Kirchhoff's law. Since clouds reduce the incoming solar radiation reaching the surface during the day and hinder the loss of terrestrial infrared radiation to space at night, cloud cover is a direct factor influencing the DTR. When cloud accumulation reaches a certain level, it leads to precipitation. Precipitation is a process in which low-temperature cloud systems from high altitudes descend to the surface, causing surface cooling, and is therefore a direct factor altering the DTR. However, weather processes such as precipitation and its timing, as well as cloud cover and its timing, involve a

considerable degree of randomness and are influenced by geographical location and seasonal variations. Not only that, but DTR is also influenced by factors such as soil moisture (Dai et al., 1999; Pyrgou, 2019), topography and vegetation (Sun D et al., 2006), and the specific location of meteorological stations, including their distance from water bodies and whether they are on the windward side (Ongoma et al., 2021). Therefore, there are bound to be exceptions to the global distribution and variations of DTR. In fact, such exceptions can be seen in Fig. 2 and Fig. 3. It should be clarified that these so-called exceptions are not due to physical mechanisms, but rather stem from the peculiarities of weather (climate).

5 Analysis of DTR Variations Based on the Radiative Characteristics of Water Vapor Condensation

5.1 Daily Variations of DTR - A Case Study of Beijing

To identify the key factors determining the characteristics of DTR variations, we should start with an understanding of its daily changes. Here, a brief analysis is presented using Beijing as a case study. Fig.4 shows the daily variations of maximum and minimum temperatures in Beijing from July 17, 2024, to August 1, 2024. The data is sourced from the National Meteorological Centre (NMC) of China (www.nmc.cn).

In Beijing, the weather was sunny with scattered clouds on July 17, clear on the 18th, and cloudy turning overcast on the 19th. From 18:00 to 22:00, the city received 5.8 mm of precipitation. On the 20th, it remained cloudy turning overcast, and on the 21st, it turned cloudy with thunder showers. From July 18th to 21st, cloud coverage was significant. Consequently, the daily maximum temperature did not rise but decreased, while the water vapor content in the atmosphere gradually increased. As conditions became more favorable for reaching the dew point temperature, phenomena such as radiation from water vapor condensation, evaporation (day) and re-condensation (night) of cloud droplets occurred repeatedly. This led to an increase in the minimum temperature (rising from 22.4℃ to 26.6℃), causing the DTR to decrease rapidly (from

15.1℃ on the 18th to 7.6℃ on the 21st). On July 22nd, it was mostly cloudy and turned cloudy during the day. The highest temperature in Beijing decreased compared to the previous day, reaching 32.2 ℃. In the evening, rain came to Beijing, and the nighttime rainfall increased slightly. Due to the overall moderate rainfall, the minimum temperature also slightly decreased, dropping from 26.6 ℃ the previous day to 23.9 ℃, and the DTR was 8.3 ℃.

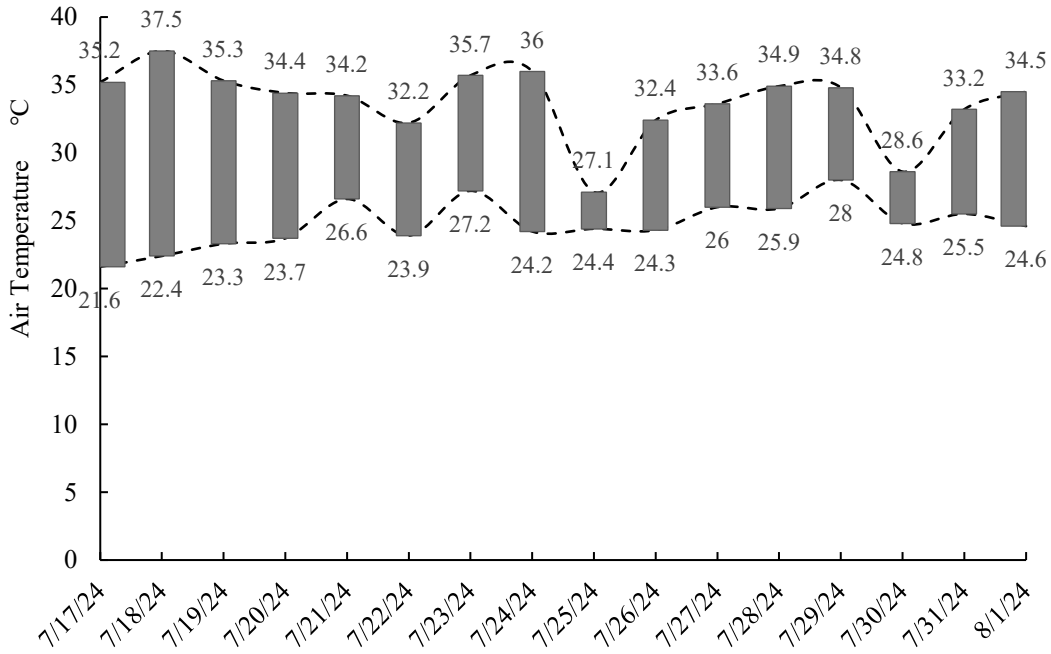

Fig. 4 Daily Variations of Maximum and Minimum Temperatures in Beijing During Summer

On the 23rd, the weather transitioned from cloudy to sunny during the day, with the maximum temperature rising to 35.7℃. The night was clear to partly cloudy, and the minimum temperature increased to 27.2℃, resulting in a DTR of 8.5℃. From 14:00 on July 24 to 19:00 on July 25, 2024, the average precipitation across Beijing was 44.7 mm. Since the precipitation began after 14:00, the maximum temperature on the 24th remained high at 36℃. However, the minimum temperature dropped from 27.2℃ on the previous day to 24.2℃, causing the DTR to rise to 11.8℃. As the precipitation continued until 19:00 on the 25th, the maximum temperature dropped significantly from 36℃ on the 24th to 27.1℃ on the 25th. Conversely, the minimum temperature

rose slightly from 24.2℃ to 24.4℃. This was due to the increased air humidity caused by precipitation and surface evaporation, which enhanced the radiative release of latent heat from water vapor condensation at night. Consequently, the DTR decreased sharply to 2.7℃. If the precipitation had started in the early morning of July 25, the minimum temperature on the 24th would likely have been higher than the previous day's 27.2℃. This is because, prior to the onset of precipitation, high air humidity maintained a persistently sultry state in Beijing. This highlights that precipitation and its timing have a direct impact on DTR variations.

Beijing experienced thunder showers on July 26, followed by cloudy weather on July 27 - 28. From 20:00 on July 29 to 14:30 on July 30, the average precipitation across Beijing was 67.0 mm. This precipitation event caused the maximum temperature on the 30th to drop from 34.8℃ on the 29th to 28.6℃, and the minimum temperature to fall from 28℃ to 24.8℃. Consequently, the DTR decreased from 6.8℃ on the 29th to 3.8℃. Compared with the previous precipitation event (July 24 - 25), this event had significantly higher precipitation volume. However, since the precipitation ended earlier, the influence of solar radiation reaching the surface was more pronounced. As a result, the reduction in maximum temperature was notably smaller, leading to a DTR on the 30th that was significantly higher than that on the 25th.

It is worth noting that in the days leading up to the two major precipitation events on July 25 and July 30, there was a progressive intensification of unusually sultry weather. This is a typical climate feature when rainstorm comes in summer, which is completely consistent with the physical mechanism that the latent heat of water vapor condensation is released in the way of radiation.

Different geographical locations possess distinct precipitation characteristics and atmospheric relative humidity levels, leading to corresponding variations in DTR. Based on the radiative characteristics of water vapor condensation, the daily variation characteristics of the DTR can be explained more clearly.

5.2 Seasonal variations of DTR

Table 1 lists the monthly average temperature (MAT), diurnal temperature range (DTR), precipitation, and relative humidity (RH) for representative cities and towns in China. These meteorological data in the table indicate that the DTR of coastal cities such as Dalian and Qingdao is lower than that of inland cities, meaning the DTR over the ocean is always lower than that over land. The Xisha Islands (low latitude) in the South China Sea have the lowest DTR. Correspondingly, the highest DTR values are found in the western interior and desert regions of China, located in the hinterland of the Eurasian continent, such as Tazhong Town in Qiemo County, Bayingolin Mongol Autonomous Prefecture, Xinjiang Uygur Autonomous Region (Note: Tazhong Town is located in the center of the Taklamakan Desert).

Comparing the data for July and January in Table 1, the DTR in summer is generally lower than in winter. At the same time, precipitation in summer is significantly higher than in winter. Furthermore, the DTR in low-latitude cities is generally lower than in high-latitude cities. As the latitude decreases from Harbin, Beijing, and Wuhan to Guangzhou, the DTR also gradually decreases. This is fully consistent with the description in Section 4 and aligns with the radiative characteristics of water vapor condensation specific to the local time and geographical conditions.

The situation in April (spring) is somewhat unique. Compared to January (winter), the MAT in all cities has increased significantly. With the exception of the Xisha Islands, monthly mean precipitation in the other cities listed in Table 1 has also increased. This increase is more pronounced in lower-latitude regions such as Wuhan and Guangzhou, where the relative humidity of the air has also risen. According to the thermodynamic properties of moist air, higher temperatures and higher relative humidity result in higher water vapor partial pressure - meaning the air contains more water vapor. Under these conditions, water vapor is more prone to reaching a state of condensation. Consequently, the potential volume of condensation increases, exerting a greater influence on the DTR. In fact, Guangzhou, located in South China (lower latitude), experiences significantly higher monthly mean precipitation in April than in January, resulting in

its highest annual relative humidity. This causes the DTR in Guangzhou in April to be lower not only than in January but also lower than in July. Conversely, for Harbin in Northeast China (higher latitude) and Beijing in North China, spring is the windy season. The lower relative humidity during this time is unfavorable for water vapor condensation; therefore, their DTR in April is actually larger than in January. Wuhan, located in Central China (mid-latitude), shows virtually no change in DTR between April and January, with data falling between that of Guangzhou and Beijing.

Since precipitation and its timing, cloud coverage and its timing, as well as the atmospheric humidity varying with these factors are influenced by geographical location and seasonal changes, weather patterns exhibit a considerable degree of randomness. Therefore, it is normal for certain exceptions to occur in the variation characteristics of the DTR. For instance, there is a significant north-south disparity in precipitation along the west coast of North America. Vancouver, located in the north, receives abundant precipitation, whereas Los Angeles and San Francisco in the south receive very little. However, they share one commonality: precipitation is lower in summer than in winter, which is characteristic of a Mediterranean climate. Under such conditions, the summer DTR is often greater than in winter; meanwhile, Vancouver in the north has a smaller DTR compared to Los Angeles and San Francisco in the south.

Table 1 Main Climate Data of Some Cities and Towns in China

Cities or Towns	Indicators	Units	Jan.	Apr.	Jul.	Oct.	Annual
	MAT	℃	-19.4	6.0	22.8	5.6	3.6
Harbin[a]	DTR	℃	11.6	13.0	9.9	11.5	11.7
126.63°E, 45.75°N	Precipitation	mm	3.7	23.8	160.7	27.6	523.3
	RH	%	74	51	77	65	67
	MAT	℃	-4.6	13.1	25.8	12.4	11.5
Beijing[a]	DTR	℃	11.2	12.9	9.3	11.9	11.4
116.47°E, 39.90°N	Precipitation	mm	3.0	19.4	192.5	24.0	644.2

	RH	%	45	48	78	66	60
	MAT	℃	-8.8	16.3	28.35	12.1	12.2
Tazhong[b]	DTR	℃	17.6	18	15.5	20.4	17.7
83.63°E, 38.07°N	Precipitation	mm	-	-	-	-	-
	RH	%	-	-	-	-	-
	MAT	℃	-3.3	11	24.1	14.5	11.6
Dalian[b]	DTR	℃	6.2	8	5.6	6.8	6.7
121.63°E, 38.90°N	Precipitation	mm	8	29.1	127.6	33.5	579.8
	RH	%	-	-	-	-	-
	MAT	℃	0.1	11.8	24.85	16.8	13.4
Qingdao[b]	DTR	℃	6	7	4.9	6.6	6.2
120.30°E, 36.07°N	Precipitation	mm	11.2	28.5	148.6	39.7	640.9
	RH	%	-	-	-	-	-
	MAT	℃	3.0	16.1	28.8	17.5	16.3
Wuhan[a]	DTR	℃	8.7	8.7	7.6	9.6	8.6
114.33°E, 30.60°N	Precipitation	mm	34.9	140.0	156.2	62.9	1204.5
	RH	%	76	81	79	77	78
	MAT	℃	13.3	17.9	28.4	23.7	21.8
Guangzhou[a]	DTR	℃	8.6	6.6	7.4	8.4	7.6
113.30°E, 23.17°N	Precipitation	mm	36.9	175.0	212.7	69.2	1694.1
	RH	%	70	85	83	73	79
	MAT	℃	22.9	27.1	28.7	26.8	26.5
Xisha[a]	DTR	℃	4.0	4.7	4.0	4.2	
112.03°E, 16.33°N	Precipitation	mm	35.2	25.5	233.9	260.6	1506.1
	RH	%	78	81	83	82	81

Notes: a. These data are from “Climate of China” by Lin Zhiguang and Zhang Jiacheng (1985).

b. These data are from the website of National Meteorological Center of China (www.nmc.cn).

According to the website of the Canadian Meteorological Agency, the seasonal variations of

MAT, DTR, and monthly mean precipitation in Vancouver and Winnipeg are shown in Table 2.

Table 2 Main Climate Data for Vancouver and Winnipeg

Cities	Indicators	Units	Jan	Apr	Jul	Oct	Annual
Vancouver 123.10°W, 49.22°N	MAT	℃	2.85	8.87	16.87	9.84	9.66
	DTR	℃	5.31	7.72	8.98	6.69	7.16
	Precipitation	mm	154.1	70.0	33.2	115.6	1123.7
Winnipeg 97.14°W, 49.90°N	MAT	℃	-17.67	3.89	19.81	5.91	2.64
	DTR	℃	9.67	11.52	12.53	10.43	11.05
	Precipitation	mm	30.4	37.4	82.2	39.8	594

Note: The data are from https://climate.weather.gc.ca.

Vancouver is at a slightly lower latitude than Winnipeg and thus receives slightly more solar radiation. The differences in temperature variations between these two cities are enormous. According to Table 2, the MAT in Vancouver in July is 2.94℃ (=19.81℃ - 16.87℃) lower than that in Winnipeg. In contrast, during the winter, the MAT in Vancouver in January is 20.52℃ (=2.85℃ - (-17.67℃)) higher than that in Winnipeg. Due to its proximity to the coast, Vancouver has more moist air and higher annual precipitation compared to Winnipeg. Consequently, the DTR in Vancouver is significantly smaller than that in Winnipeg, which is consistent with the radiative characteristics of water vapor condensation.

In Vancouver, the monthly mean precipitation decreases as the seasons warm, leading to an increase in the DTR. In contrast, Winnipeg experiences an increase in the monthly mean precipitation with seasonal warming, yet its DTR rises instead of falling, which appears somewhat anomalous. To explain this phenomenon, we compare it with Harbin in northeastern China. Both Winnipeg and Harbin are inland cities, with Winnipeg at a slightly higher latitude than Harbin. As a result, Winnipeg receives slightly less solar radiation than Harbin. However, Winnipeg's MAT in January is higher than that of Harbin, and its monthly mean precipitation is significantly

greater, leading to a lower DTR compared to Harbin. In contrast, during the summer, Winnipeg's MAT is lower than Harbin's, and its monthly mean precipitation is only slightly more than half that of Harbin. Consequently, the air in Winnipeg is much drier. This is a key reason why Winnipeg's summer DTR is higher than its winter DTR and exceeds that of Harbin.

In fact, since lower temperatures result in a reduced capacity of the atmosphere to hold water vapor, the amount of water vapor in the atmosphere is typically very low under the low-temperature conditions of winter in high-latitude regions. As warming occurs from winter to summer, the atmosphere in inland cities may experience very low relative humidity due to a temporary insufficiency of water vapor sources. In other words, the air in many high-latitude inland cities is driest during the spring. Due to the limited increase in precipitation in Winnipeg in July compared to January, and its relatively low MAT (only 19.81℃), the climatic characteristics of the city at this time resemble spring rather than summer.

From winter to summer, surface evaporation significantly increases, and precipitation usually follows suit. However, this is not the case in some regions, such as the Mediterranean, western and coastal areas of the United States (Sun D et al., 2006), central Chile, and many cities in southwestern Europe (Katavoutas et al., 2023). In almost all areas with such climatic characteristics, the DTR in summer is typically higher than in winter, making them exceptions to the global trend of decreasing summer DTR.

Of course, there are also cities or regions that fall somewhere in between the aforementioned scenarios, such as Nice in France and Barcelona in Spain (Katavoutas et al., 2023), where seasonal variations are weak and the annual DTR fluctuation is minimal. Among the Chinese cities not listed in Table 1, there are also many exceptions. Since all these exceptions are related to the radiative characteristics of water vapor condensation specific to the local time and geographical conditions, the arguments presented in this paper are objective and valid.

5.3 Annual variations of DTR under the background of global warming

According to the IPCC Third Assessment Report: "The overall global trend for the maximum

temperature during 1950 to 1993 is approximately 0.1℃/decade and the trend for the minimum temperature is about 0.2℃/decade. Consequently, the trend in the DTR is about -0.1℃/decade (Folland et al., 2002).” However, special attention is drawn to the issue of “restricted data coverage”, and explanations were provided regarding the inconsistent distribution of DTR changes across different countries and regions. In his monograph *Climate Processes and Climatic Change*, Australian scholar Edward Bryant (1997) stated that almost all surface warming over land is attributable to rising nighttime temperatures - i.e., a significant decrease in DTR - which is largely consistent with the conclusions of the IPCC Third Assessment Report. Although the increase in carbon dioxide concentration is a well-known fact, the IPCC Third Assessment Report also provided data on increased precipitation: “Widespread increases are likely to have occurred in the proportion of total precipitation derived from heavy and extreme precipitation events over land in the mid- and high latitudes of the Northern Hemisphere” (Folland et al., 2002).

The decline in DTR observed over global land surfaces from the 1950s to the 1980s has been confirmed in AR4, AR5, and AR6. AR4 revealed that there was no change in DTR from 1979 to 2004, as daytime and nighttime temperatures rose at roughly the same rate (Solomon et al., 2008). AR5 explained that “the observed decline in DTR over global land surfaces from the 1950s to the 1980s, and its stabilization thereafter fits to a large-scale dimming and subsequent brightening, respectively (Folland et al., 2013).” “The Technical Summary of AR4 highlighted changes in DTR and their causes as a key uncertainty. Since AR4, uncertainties in DTR and its physical interpretation have become even more apparent (Folland et al., 2013).” According to IPCC Sixth Assessment Report (AR6): “There is a considerable degree of ambiguity in estimates prior to 1950 due to sparse data availability. Estimates after 1950 unanimously agree that global DTR has declined, with most of the decline occurring between 1960 and 1980 (Gulev et al., 2021; Thorne et al., 2016b; Sun et al., 2019).” Correspondingly, “precipitation on land has also increased since the mid-1950s. Since the 1970s, the near surface humidity (i.e. water vapor) on land has been increasing (Gulev et al., 2021).”

Global warming is an indisputable fact. However, accompanying global warming, the DTR has changed accordingly: “Since 1900, global DTR has declined significantly at 0.025 ± 0.006℃ per decade, with a slight increase from 1900 to 1950 and a modest decline of 0.016 ± 0.015℃ per decade since 1950. However, DTR trends shifted to significant increases of 0.063 ± 0.021℃ per decade since 1979 and 0.136 ± 0.037℃ per decade since 1998, reflecting complex changes (Xu et al., 2025).” “Notable differences and uncertainties remain across data sets due to variations in data sources, coverage, and processing methods (Xu et al., 2025).” Regardless of how the DTR changes, it is highly correlated with precipitation levels: “there is a significant negative correlation between precipitation and DTR in the Northern Hemisphere (NH), with a correlation coefficient of -0.61. Precipitation in the NH decreased before the early 1950s, while the trend after the early 1950s has increased. Overall, precipitation data could strongly support the DTR reversal phenomenon occurring around the 1950s (Sun et al., 2019).”

The negative correlation between annual DTR variations and precipitation is underpinned by the radiative characteristics of nighttime water vapor condensation. The insufficiency of precipitation is associated with an increase in high DTR extreme events (He et al., 2015), which conversely validates the analysis presented in this paper. Evidently, only based on the physical mechanism of condensation radiation can the global distribution and variation of DTR be reasonably explained.

6 Conclusions

This paper establishes that the radiative release of latent heat from water vapor condensation is the dominant factor governing the global distribution and variation of DTR. We resolve the thermodynamic paradox in classical cloud physics: in the absence of a conductive temperature gradient, phase transition radiation is the sole pathway for energy dissipation. Evidence from atmospheric infrared anomalies and precipitation-related UHF signals supports this mechanism.

Our analysis confirms that DTR is inversely correlated with condensation intensity. Regions

with abundant moisture (coasts, low latitudes, summers) exhibit smaller DTR due to enhanced nighttime radiative heating, while arid regions (inland, high latitudes, winters) show larger DTR. This explains historical DTR trends, including the asymmetric warming of minimum temperatures and the stabilization of DTR post-1980s linked to global dimming/brightening cycles. Exceptions in Mediterranean climates further validate the model's sensitivity to local precipitation seasonality.

Future climate research must integrate condensation radiation into energy budget models, replacing the invalid assumption of the atmosphere as a passive heat reservoir. This paradigm shift is essential for accurately predicting regional climate responses and addressing the uncertainties highlighted by the IPCC.

References

Andrews DG. 2010. An Introduction to Atmospheric Physics, 2nd Edition. Cambridge University Press. 237pp. Doi: 10.1017/CBO9780511800788.

Barkan J, Shafir H, Alpert P. 2020, Multi-factor Analysis of DTR Variability over Israel in the Sea/Desert Border. Theoretical & Applied Climatology, 139(13). Doi: 10.1007/s00704-019-02958-x.

Bryant E. 1997. Climate Process & Change, Cambridge University Press, 209pp. Doi: 10.1017/CBO9781139166751.

Dai A, Trenberth K E, Karl T R. 1999. Effects of Clouds, Soil Moisture, Precipitation, and Water Vapor on Diurnal Temperature Range. J Climate, 12: 2451-2473. Doi: 10.1175 /1520 0442(1999)012%3c2451: EOCSMP% 3e2.0.CO;2.

Gulev S K, Thorne P W, Ahn J, Dentener F J, et al. 2021. Changing State of the Climate System. In Climate Change 2021: The Physical Science Basis. Contribution of Working Group I to the Sixth Assessment Report of the Intergovernmental Panel on Climate Change. Cambridge University Press, Cambridge, United Kingdom and New York, USA, 2021: 287-422. Doi: 10.1017/9781009157896.004.

Hartmann D L, Albert M G, et al. 2013. Observations: Atmosphere and Surface, in Climate Change 2013: The Physical Science Basis. Contribution of Working Group I to the Fifth Assessment Report of the Intergovernmental Panel on Climate Change: 159-254, Cambridge University Press, Cambridge, UK and New York, USA, 2013, Doi: 10.1017/ CBO9781107415324.008.

He B, Huang L, Wang Q. 2015. Precipitation Deficits Increase High Diurnal Temperature Range Extremes. Scientific Reports, 5(1), 12004. Doi: 10.1038/srep12004.

Janna WS. 2009. Engineering Heat Transfer, 3rd Edition. Boca Raton: Taylor & Francis Group, 692pp. ISBN: 9781000055030.

Karl TR, Jones PD, Knight, RW, Kukla, G, et al. 1993. A New Perspective on Recent Global Warming: Asymmetric Trends of Daily Maximum and Minimum Temperature. Bulletin of the American Meteorological Society, 74(6), 1007–1024. Doi:

10.1175/1520-0477(1993)074<1007:ANPORG>2.0.CO;2.

Katavoutas G, Founda D, Varotsos K V, Giannakopoulos C. 2023. Diurnal Temperature Range and Its Response to Heat Waves in 16 European Cities -Current and Future Trends. Sustainability, 15, 12715. Doi: 10.3390/su151712715.

Kiehl J T and Trenberth K E. 1997. Earth's Annual Global Mean Energy Budget, Bulletin of the American Meteorological Society, 78, 197-208. Doi: 10.1175/1520-0477(1997) 078<0197:EAGMEB>2.0.CO;2.

Klimenko, VV and Mareev, EA. 2018. Anomalous Decimeter Radio Noise from the Region of the Atmospheric Front: I. Characteristics of the Detected Radio Noise and Meteorological Parameters of the Frontal Cloudiness. Izvestiya Atmospheric and Oceanic Physics, 54(2): 147-153. Doi: 10.1134/S0001433818020135.

Lin Zhiguang and Zhang Jiacheng. 1985. Climate of China (in Chinese). Shaanxi Province (China): Xi'an: Shaanxi People Press. 450pp.

Makowski K, Wild M and Ohmura A. 2008. Diurnal Temperature Range over Europe between 1950 and 2005, Atmospheric Chemistry and Physics, 8: 6483–6498, Doi: 10.5194/acp-8-6483-2008.

Manabe S, Wetherald R T. 1967. Thermal Equilibrium of the Atmosphere with a Given Distribution of Relative Humidity. Journal of Atmospheric Sciences. 24(3): 241-259. Doi: 10.1175/1520-0469(1967)024<0241: TEOTAW>2.0.CO;2.

Mason BJ. 1975. Clouds, Rain and Rainmaking, 2nd Edition. Cambridge University Press. 189pp.

Mestvirishvili AN, Directovich JG, Grigoriev SI, Perel'man ME. 1977. Characteristic radiation due to the phase transitions latent energy. Physics Letters A. 60(2), 143-144. Doi: 10.1016/0375-9601(77)90409-1.

Ongoma V, Rahman MA, Ayugi B, et al. 2021. Variability of Diurnal Temperature Range over Pacific Island Countries, A Case Study of Fiji, Meteorology and Atmospheric Physics, 133: 85-95, Doi: 10.1007/s00703-020-00743-4.

Perel'man ME, Tatartchenko VA. 2008. Phase Transitions of the First Kind as Radiation Processes. Physics Letters A, 372(14): 2480-2483. Doi: 10.1016/j.physleta.2007.11.056.

Potter W R, Hoffman J G. 1968. Phase Transition Luminescence in Boiling Water: Evidence for Clusters. Infrared Physics. 8: 265-270. Doi: 10.1016/0020-0891(68)90035-3.

Sall SA and Smirnov AP. 2000. Phase-Transition Radiation and the Growth of a New Phase. Technical Physics, 45(7): 849 - 853. Doi: 10.1134/1.1259737.

Solomon S, Qin D, Manning M, Chen Z, et al. 2008. Climate Change 2007: The Physical Science Basis. Contribution of Working Group I to the Fourth Assessment Report of the Intergovernmental Panel on Climate Change. Cambridge University Press, Cambridge, United Kingdom and New York, NY, USA, 996pp. ISBN 978 0521 88009-1.

Stocker TF, Clarke GKC, et al., 2002, Physical Climate Processes and Feedbacks. In Climate Change 2001: The Scientific Basis. Contribution of Working Group I to the Third Assessment Report of the Intergovernmental Panel on Climate Change. Cambridge University Press, Cambridge, United Kingdom and New York, USA: 417-470. ISBN 0521 80767 0.

Sun D, Kafatos M, Pinker RT and Easterling DR. 2006 Seasonal Variations in Diurnal Temperature Range from Satellites and Surface Observations. IEEE Transactions on Geoscience and Remote Sensing, 44(10): 2779 - 2785, Doi: 10.1109/TGRS.2006.871895.

Sun X, Ren G, You Q, Ren Y, et al. 2019. Global Diurnal Temperature Range (DTR) Changes since 1901. Clim Dyn, 52: 3343

- 3356. Doi: 10.1007/s0038 2-018-4329-6.

Sun X, Wang C, Ren G. 2021. Changes in the Diurnal Temperature Range over East Asia from 1901 to 2018 and Its Relationship with Precipitation. Climatic Change, 166: 44(1-17). Doi: 10.1007/s10584-021-03120-1.

Tatartchenko VA, 2008. Characteristic IR radiation accompanying crystallization and window of transparency for it. Journal of Crystal Growth, 310: 525 - 529. Doi: 10.1016/j.jcrysgro.2007.11.155.

Tatartchenko VA, 2010. Infrared characteristic radiation of water condensation and freezing in connection with atmospheric phenomena. Earth-Science Reviews, 101: 24 - 28. Doi: 10.1016/j.earscirev.2010.03.002.

Tatartchenko V, Liu Y, Chen W, Smirnov P. 2012. Infrared characteristic radiation of water condensation and freezing in connection with atmospheric phenomena; Part 3: Experimental data. Earth-Science Reviews. 114: 218–223. Doi: 10.1016/j.earscirev.2012.07.001

Thorne PW, Menne M J, Williams C N, et al. 2016a. Reassessing Changes in Diurnal Temperature Range: A New Data Set and Characterization of Data Biases. Journal of Geophysical Research: Atmospheres, 121(10), 5115–5137, Doi: 10.1002 /2015jd024583.

Thorne PW, Menne M J, Williams C N, et al. 2016b. Reassessing Changes in Diurnal Temperature Range: Intercomparison and Evaluation of Existing Global Data Set Estimates, Journal of Geophysical Research: Atmospheres, 121(10), 5138–5158, Doi: 10.1002/2015jd024584.

Vinnarasi R, Dhanya C T, Chakravorty A, Aghakouchak A. 2017. Unravelling Diurnal Asymmetry of Surface Temperature in Different Climate Zones. Scientific Reports, 7(1): 1-8. Doi: 10.1038/s41598-017-07627-5.

Xu Q, Wei S, Li Z, Li Q. 2025. A New Evaluation of Observed Changes in Diurnal Temperature Range, Geophysical Research Letters, 52(2): 1-12. Doi: 10.1029/2024GL113406.

Wang PK. 2013. Physics and Dynamics of Clouds and Precipitation, Cambridge University Press, 478pp. ISBN 9781107306318.

Wang K and Brewster QM. 2010. Phase-transition radiation in vapor condensation process. International Communications in Heat and Mass Transfer, 37: 945-949. Doi: 10.1016/j.icheatmasstransfer.2010.06.019.

Zhou Shaoxiang. 2008. Oppugning the Condensation Growth Equation of Cloud Droplets (in Chinese). Desert and Oasis Meteorology. 2(4): 55-59.